MmBack: Clock-free Multi-Sensor Backscatter with Synchronous Acquisition and Multiplexing

Yijie Li
National University of Singapore
yijieli@nus.edu.sg

Weichong Ling
National University of Singapore
wling@u.nus.edu

Taiting Lu
Pennsylvania State University
txl5518@psu.edu

Yi-Chao Chen
Shanghai Jiao Tong University
yichao@sjtu.edu.cn

Vaishnavi Ranganathan
Microsoft Research
Vaishnavi.Ranganathan@
microsoft.com

Lili Qiu
UT Austin, MSR Asia Shanghai
liliqiu@microsoft.com

Jingxian Wang
National University of Singapore
wang@nus.edu.sg

ABSTRACT

Backscatter tags provide a low-power solution for sensor applications, yet many real-world scenarios require multiple sensors—often of different types—for complex sensing tasks. However, existing designs support only a single sensor per tag, increasing spatial overhead. State-of-the-art approaches to multiplexing multiple sensor streams on a single tag rely on onboard clocks or multiple modulation chains, which add cost, enlarge form factor, and remain prone to timing drift—disrupting synchronization across sensors.

We present MmBack, a low-power, clock-free backscatter tag that enables synchronous multi-sensor data acquisition and multiplexing over a single modulation chain. MmBack synchronizes sensor inputs in parallel using a shared reference signal extracted from ambient RF excitation, eliminating the need for an onboard timing source. To efficiently multiplex sensor data, MmBack designs a voltage-division scheme to multiplex multiple sensor inputs as backscatter frequency shifts through a single oscillator and RF switch. At the receiver, MmBack develops a frequency tracking algorithm and a finite-state machine for accurate demultiplexing. Mm-Back's ASIC design consumes $25.56\mu W$, while its prototype supports 5 concurrent sensor streams with bandwidths of up to $5kHz$ and 3 concurrent sensor streams with bandwidth of up to $18kHz$. Evaluation shows that MmBack achieves an average SNR surpassing $15dB$ in signal reconstruction.

1 INTRODUCTION

RF-based backscatter devices have emerged as a low-power solution for sensor applications by backscattering sensed data onto ambient wireless signals. However, existing backscatter tags [1, 6, 35, 40, 43, 43, 53, 66, 67] support only a single sensor, limiting them to one sensing modality per tag (e.g., temperature [39] or muscle stretch [52]). Yet, real-world applications often require multi-modal sensing, particularly for complex monitoring tasks such as soil nutrient evaluation [9, 59], plant stress detection [4, 30, 32, 64], and human health tracking [29]. For example, [32] highlights the need for attaching four sensors—including humidity, optical, and temperature—onto a single leaf to improve plant stress detection. Despite this need, current backscatter solutions remain constrained to single-sensor-per-tag configurations.

This work aims to develop a backscatter tag capable of streaming multiple sensor readings. A natural approach is frequency-division multiplexing (FDM), where each sensor stream backscatters over a distinct frequency band—a potential extension of existing work [40]. However, FDM requires independent modulation chains on a single tag, each with its own oscillator and mixer for frequency shifting, significantly increasing hardware complexity and tag size. Recent work [68] explored time-division multiplexing (TDM) by sequentially polling multiple microphone sensors on the same tag, but this requires a costly FPGA—driving per-tag costs over 500$ [16]. Moreover, TDM relies on an onboard clock for polling and synchronization, making it vulnerable to clock drift caused by crystal oscillator instability—particularly in low-power, low-cost clocks [10, 22, 23]. This drift, accumulating to several *ms* over hours [41], degrades performance in timing-sensitive tasks like ultrasonic tracking [18, 31, 51, 65], where precise synchronization between sensors is critical. While actively synchronizing the tag's onboard clock with the external infrastructure (e.g., the reader) can partially mitigate drift, it adds computational and hardware complexity to the tag. Thus, there remains a gap for a low-power, low-cost backscatter tag that enables synchronous multi-sensor data acquisition and multiplexing over a single modulation chain—without requiring an onboard clock.
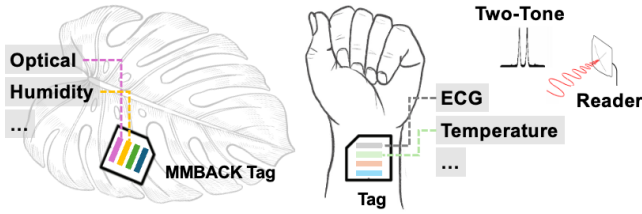
Figure 1: General-purpose MmBack backscatter interface enables synchronous data acquisition from multiple sensors and multiplexes sensor inputs onto the backscattered signal without an onboard clock. The reader transmits a two-tone carrier, allowing the tag to backscatter data while extracting a timing reference.

We present MmBack, a low-power, low-cost, clock-free backscatter sensing interface that enables synchronous signal acquisition and multiplexing using a single modulation chain from multiple off-the-shelf sensors (Fig. 1). Unlike existing designs that rely on sequential polling with an onboard clock, MmBack synchronizes all sensor inputs in parallel using a shared reference signal, extracted directly from ambient RF excitation—eliminating the need for an onboard clock. The synchronous signals are then multiplexed via MmBack's novel voltage-division scheme and backscattered as frequency shifts through a single modulation chain. At the receiver, MmBack designs a frequency tracking algorithm, leveraging a series of Chirp-Z Transforms for accurate reconstruction of individual sensor signals. MmBack operates in the $915MHz$ ISM band, consuming 25.56 μW. Our PCB prototype supports up to five sensors. Through extensive experiments, we demonstrate that MmBack achieves an average SNR over $15dB$ in signal recovery, supporting input sensor signals with bandwidths of up to 50 kHz for three sensors and up to 10 kHz for five sensors.

The first objective of MmBack is to achieve synchronous data acquisition from multiple sensor streams without relying onboard clocks. Traditional designs [35, 68] rely on precise onboard clocks, increasing hardware cost and are susceptible to clock drift. To address this, MmBack introduces a novel clock-free synchronous sensor reading module that encodes multiple sensor inputs in a parallel architecture. By leveraging parallel micro-power comparators referenced to a shared sawtooth waveform, MmBack concurrently encodes multiple sensor streams into Pulse Width Modulation (PWM) signals. Instead of using an onboard clock, MmBack builds a low-power circuit that derives a stable sawtooth reference signal directly from ambient RF excitation. Specifically, this is achieved by extracting the envelope of a two-tone RF signal to generate a differential frequency timing reference. To maintain stability in dynamic radio environments like multipath fading, MmBack employs a comparator to extract a

timing reference that remains resilient to environmental interference. Additionally, MmBack incorporates a constant current source circuit with a potentiometer, allowing on-the-fly adjustment of the sawtooth frequency to match varying sensor requirements without hardware modifications.

Next, MmBack focuses on multiplexing all sensor streams onto a backscatter signal using a single modulation chain, while ensuring that each sensor remains distinguishable and decodable. Traditional FDM approaches require separate oscillators and mixers for each sensor, increasing hardware complexity and tag size. Instead, MmBack presents a novel voltage-division multiplexing scheme (VDM) that encodes multiple inputs into a single composite voltage signal, which can then be modulated through a single modulation chain. Key to MmBack's novel multiplexing design is assigning each sensor a unique voltage contribution following a binary-weighted geometric progression, ensuring that every combination of sensor signals produces a distinct and decodable voltage level. This geometric progression assignment also ensures uniform voltage spacing, enhancing the receiver's reliability to distinguish sensor signals. By leveraging this design, MmBack efficiently multiplexes multiple synchronized sensor streams using only a oscillator and an RF switch, significantly reducing hardware overhead while maintaining signal integrity.

Once sensor signals are multiplexed onto the backscatter signal, MmBack's receiver must demultiplex them into individual sensor signals. This requires detecting both backscatter frequency changes and their exact timing. To achieve this, MmBack applies a series of Chirp-Z Transform (CZT) to densify spectral representation and capture transient frequency shifts by analyzing variations across consecutive CZT spectrums. Furthermore, we implement a finite state machine (FSM) algorithm to track frequency transitions in a structured manner, increasing both efficiency and robustness.

We implement MmBack's prototype on a two-layer PCB with commercial off-the-shelf components. The prototype has a compact form factor ($3cm$ by $2cm$) and costs $17 per tag, interfacing up to five sensors. The ASIC design of MmBack consumes 19.32 μW for signal multiplexing and 7.47 μW for reference signal extraction. With a preliminary two-layer PCB prototype, power consumption varies between $1.36mW \sim 2.32mW$, depending on the number of sensors (1 to 6). MmBack operates in the 915 MHz UHF band, using an excitation signal transmitted from a USRP B210. We evaluate MmBack's sensing interface with 9 different sensor types and test across applications, including plant sensing, acoustic AoA estimation, and human health monitoring. Experiments are conducted in both line-of-sight and non-line-of-sight scenarios, as well as in environments with moving objects. Our results show that:

- MmBack achieves an average SNR of over 15 dB in signal recovery, and supports input sensor signals with bandwidths of up to 18 kHz for three sensors and up to 5 kHz for five sensors.
- MmBack achieves a synchronization accuracy of 2 ns across sensor streams.
- MmBack achieves an acoustic AoA estimation error of $3.6°$ for a 1 kHz wave and $11.7°$ for a 5 kHz wave. It also shows high signal recovery quality in plant sensing and human health monitoring tasks.

Contributions: MmBack's core contributions include:
- A multi-sensor backscatter interface that supports synchronous data acquisition without an onboard clock.
- A voltage-division multiplexing scheme that encodes multiple sensor signals modulated into frequency shifts using a single modulation chain.
- A passive clock-free timing reference module that extracts timing directly from ambient RF excitation.
- A decoding algorithm with differential CZT trace extraction and FSM for reconstructing sensor signals.
- Detailed evaluation with various sensor applications, e.g., timing-sensitive tasks like acoustic AoA estimation.

2 RELATED WORK

RFID-based Sensing: RFID tags [44] have been widely studied for object identification [21, 42, 48, 62, 63], localization [7, 8, 53, 57, 58, 61], and motion tracking applications [19, 25, 27, 46, 52]. By leveraging the antenna impedance coupling effects, RFID tags extend beyond location tracking to detect material property changes. Recent studies demonstrated material identification [56, 60], humidity and temperature sensing [28, 38, 39, 55], and even more complex applications such as monitoring egg incubation [50], fruit ripeness [26], gas [49], pesticide [20] by integrating various functional materials [20, 49, 54, 56, 59, 60] into the antenna. However, they are typically designed for task-specific applications, with each implementation tailored to a single sensing modality. In contrast, MmBack presents a general-purpose backscatter interface that supports various multi-modal sensing.

Customized Backscatter Sensor Interface: Researchers have built general-purpose platforms capable of interfacing with off-the-shelf sensors. Early work, such as WISP [43], uses an onboard micro-controller for programmability and an ADC for sensor data acquisition. However, these digital components are power hungry, causing WISP to consume over $1mW$ even when supporting only a single sensor. While recent studies [1, 6, 35, 40, 43, 53, 66, 67] offloaded computation-intensive signal processing to the reader to reduce power consumption, they still support only a single sensor per tag, increasing spatial and hardware overhead

Table 1: Comparison of MmBack and existing work.

System	Multi-Sensor	Synchronous	General-Purpose
ZenseTag [6]	✕	✕	✕
Wang et al. [54]	✕	✕	✕
Leggiero [35]	✕	✕	✓
WiTag [1]	✕	✕	✓
RF-bandaid [40]	✕	✕	✓
WISP [43]	✕	✕	✓
M.A.B [68]	✓	✕	✕
Mandal et al. [33]	✓	✓	✕
MmBack (ours)	✓	✓	✓

for multi-sensor applications. Instead, MmBack 's platform supports streaming multiple onboard sensors and consumes less than $1.36 \sim 2.32mW$ while interfacing with 5 sensors, and its ASIC design consumes just 25.56 μW.

Multi-Sensor Backscatter: Simultaneous multi-sensor data acquisition are essential in many complex monitoring tasks, such as soil nutrient evaluation [9, 59], plant stress monitoring [4, 30, 32, 64], and human health tracking [29]. For example, as suggested in [32], integrating multiple sensors to concurrently capture humidity, temperature, and optical data enhances plant stress assessment. While recent backscatter-based body sensing work [33] supports simultaneous multi-sensor readings, it is limited to detecting spike events and is specifically designed for monitoring signals with spike-like features (e.g., Phonocardiogram (PCG) and Phonocardiogram (PPG)). Additionally, microphone array backscatter (M.A.B) [68] explores multi-track audio transmission using backscatter but relies on time-division multiplexing (TDM) scheme to sequentially sample each track, causing $> 5\mu s$ inter-channel delay. Moreover, it requires a high-performance FPGA for logic control, driving system costs exceeding 500\$.

Table. 1 highlights MmBack, a clock-free, general-purpose backscatter tag enabling synchronous data acquisition and multiplexing from multiple sensors. MmBack supports high-bandwidth signals streaming up to $20kHz$, expanding potential for advanced applications.

3 OVERVIEW

MmBack aims to enable clock-free, synchronous multi-sensor data acquisition and multiplexing on a single backscatter tag. MmBack achieves this by (1) extracting a shared timing reference from ambient RF excitation instead of using an onboard clock, (2) multiplexing multiple sensor streams onto a single modulation chain through a voltage-division scheme, and (3) developing a frequency tracking algorithm for signal demultiplexing at the receiver.

At a high level, MmBack's system design is as follows (see Fig. 2): Sensor signals are first converted into synchronized Pulse Width Modulation (PWM) signals using a shared saw-tooth reference. These PWM signals are then multiplexed
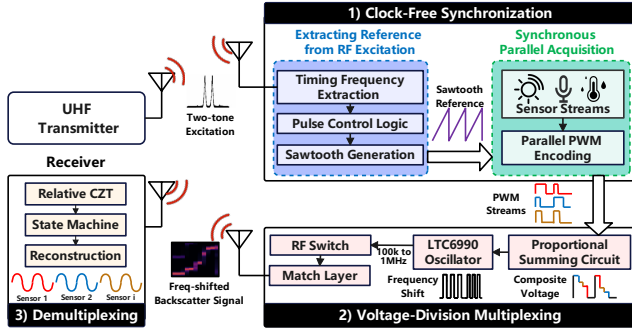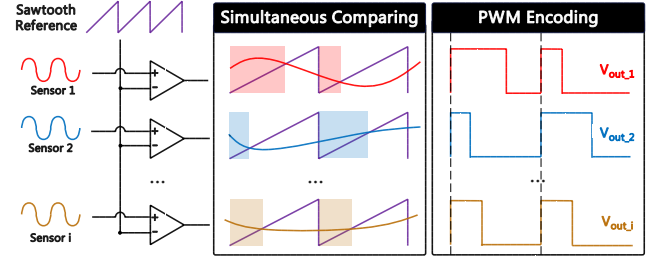
Figure 2: System Overview.

Figure 3: MMBACK encodes sensor readings into synchronized PWM signals by comparing them against a shared sawtooth reference using parallel comparators.

into a composite voltage signal based on a binary-weighted voltage-division scheme and fed into a single VCO and RF switch, which translates them into frequency shifts modulated onto the backscattered RF signal. At the receiver, the system demodulates these frequency shifts, applies a series of Chirp-Z Transforms for frequency tracking, and reconstructs individual sensor signals using a finite-state machine (FSM)-based decoding algorithm. The rest of the paper addresses the following technical challenges:

(1) Clock-Free Synchronous Sensor Data Acquisition: The key challenge is achieving precise synchronization across sensor streams without an onboard clock, which traditionally introduces drift over time. MMBACK resolves this by extracting a timing reference directly from ambient RF excitation, ensuring low-jitter (~2 nanoseconds) synchronization across all sensor inputs. Sec. 4 describes our approach.

(2) Voltage-Division Multiplexing: A major challenge in multiplexing multiple signals over a single modulation chain is ensuring that each sensor remains uniquely distinguishable. MMBACK addresses this by designing a binary-weighted voltage-division multiplexing scheme, where each sensor's voltage contribution follows a geometric progression. This ensures that every unique sensor combination produces a distinct summed voltage with uniform spacing, enhancing decoding accuracy at the receiver. Sec. 5 details our approach.

(3) Signal Demultiplexing: The challenge at the receiver lies in accurately tracking rapid backscatter frequency shifts within a constrained time window, especially for high-bandwidth signals (e.g., ultrasonic sensing). MMBACK builds a frequency tracking algorithm by leveraging a series of Chirp-Z Transform, combined with a finite-state machine based algorithm to reliably extract sensor signals. Sec. 6 details our approach.

4 CLOCK-FREE SYNCHRONOUS SENSOR READINGS

While recent work [68] integrates multiple microphone sensors on a single tag, it uses sequential polling, which requires a precise onboard clock to maintain a paced polling schedule.

This not only increases hardware cost but also introduces clock drift, causing timing misalignment between sensors. To address this, MMBACK processes all sensor streams in a parallel architecture and synchronizes across sensors using a shared reference signal (Sec. 4.1), extracted from the ambient RF excitation without using an onboard clock (Sec. 4.2).

4.1 Synchronous Parallel Acquisition

The first objective of MMBACK is to enable simultaneous and synchronized data acquisition across multiple sensor streams. To achieve this, MMBACK first encodes sensor readings into a unified time-domain representation—Pulse Width Modulation (PWM). This is accomplished using a parallel architecture, where each sensor's analog voltage is compared against a shared sawtooth reference signal using a low-power comparator (Fig. 3). Since all sensor signals are processed against a shared reference waveform, the resulting PWM signals naturally remain synchronized. The following sections detail the process of PWM signal generation and how MMBACK ensures synchronization across sensor streams.

PWM Encoding: MMBACK encodes all sensor input signals as PWM signals, where the duty cycle represents the measured value. This encoding reduces the dependency on absolute signal amplitudes, instead capturing information in a time-domain parameter—the duty cycle. Such a transformation simplifies processing and enables a structured multiplexing scheme discussed in Sec. 5.

To encode the sensor signal into a PWM, each sensor stream is compared against a sawtooth reference signal using a comparator. When the sensor voltage exceeds the voltage of the rising sawtooth waveform, the comparator outputs a high voltage; otherwise, it remains low (see details in Fig. 3). This linear rising slope allows the comparator to generate a PWM signal where the duty cycle is proportional to the sensor's analog voltage, effectively encoding the original sensor readings. Assuming the input signal's amplitude of the ith sensor stream is V_i, and the sawtooth waveform has
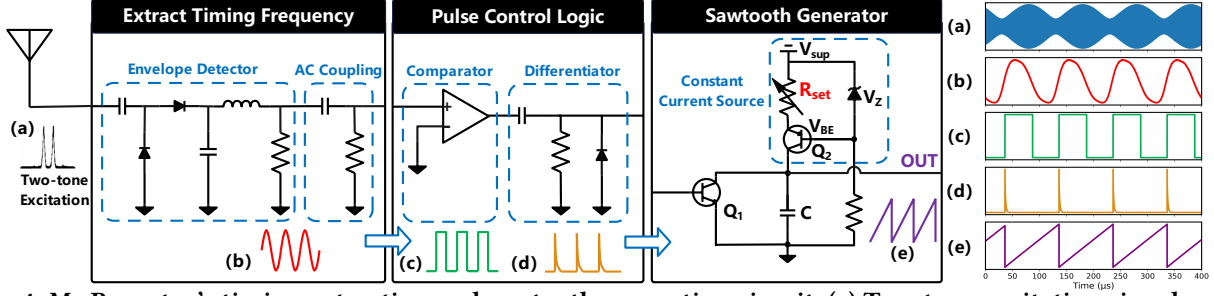
Figure 4: MmBack tag's timing extraction and sawtooth generation circuit: (a) Two-tone excitation signal received by the tag. (b) Extraction of timing frequency. (c) Generation of a square wave independent of amplitude variations. (d) Narrow pulses serving as timing markers for the sawtooth waveform. (e) Sawtooth waveform generation with on-the-fly timing frequency adaptation using a tunable resistor.

a maximum amplitude V_{max} and frequency f_s, the resulting PWM duration T_{d_i} is given by:

$$T_{d_i} = \frac{V_i}{V_{max}} \cdot \frac{1}{f_s} + \epsilon \qquad (1)$$

where ϵ is a constant delay (less than 2ns jitter) introduced by the comparator [24]. The generated PWM signals have varying duty cycles with a fixed voltage V_s.

Parallel Architecture for Synchronous Acquisition: Mm-Back achieves simultaneous and synchronized sensor readings by employing a parallel set of comparators, each referenced to the same sawtooth signal. Fig. 3 shows this parallel architecture. This ensures that all sensor inputs are processed concurrently, generating synchronized PWM signals. With a propagation delay skew of less than 2 ns [24] introduced by the comparator, MmBack maintains minimal synchronization error across sensor streams.

4.2 Extracting Reference from RF

MmBack synchronizes sensor streams by comparing each input against a shared sawtooth reference signal. Traditionally, generating a common reference requires an onboard clock, which add cost, operates at a fixed frequency, and introduces clock drift—leading to synchronization errors over time, especially across multiple tags. To overcome these limitations, MmBack extracts a timing frequency reference directly from an RF excitation source without the use of an onboard clock.

Extracting a Timing Frequency from Ambient RF: Mm-Back derives its timing frequency directly from an RF excitation source transmitting a two-tone RF signal at angular frequencies ω_1 and ω_2. The received signal $r(t)$ at the Mm-Back tag is given by:

$r(t) = \alpha_1 A \cos(\omega_1 t + \phi_1) + \alpha_2 A \cos(\omega_1 t + \phi_2)$

$= A \cos\left(\frac{\omega_1 + \omega_2}{2}t\right) \left[\alpha_1 \cos\left(\frac{\omega_1 - \omega_2}{2}t + \phi_1\right) + \alpha_2 \cos\left(-\frac{\omega_1 - \omega_2}{2}t + \phi_2\right)\right]$

$+ A \sin\left(\frac{\omega_1 + \omega_2}{2}t\right) \left[\alpha_1 \sin\left(\frac{\omega_1 - \omega_2}{2}t + \phi_1\right) - \alpha_2 \sin\left(-\frac{\omega_1 - \omega_2}{2}t + \phi_2\right)\right]$

$$\qquad (2)$$

where A is the transmitted signal amplitude, α_1 and α_2 are the attenuation coefficients, and ϕ_1 and ϕ_2 are phase shifts for each tone, respectively. Fig. 4 (a) shows the two-tone excitation signal received by the tag.

With Eqn. 2, the envelope of the received signal can be derived as

$$r_{env}(t) = A\sqrt{\alpha_1^2 + \alpha_2^2 + 2\alpha_1\alpha_2 \cos\left[(\omega_1 - \omega_2)t + (\phi_1 - \phi_2)\right]} \qquad (3)$$

Eqn. 3 shows that the envelope oscillates at the frequency difference between the two tones $f_{env} = \frac{|\omega_1 - \omega_2|}{2\pi}$. This frequency remains stable at f_{env} and can serve as a reliable timing frequency for the MmBack tag. Moreover, by adjusting the frequency separation between the two tones, f_{env} can be dynamically controlled, allowing MmBack to adapt its timing to different sensor applications. To extract f_{env}, MmBack uses a cascaded rectifier followed by a low-pass filter, as shown in Fig. 4 (b).

Accounting for Dynamic Radio Environments: The envelope amplitude and DC offset of the received signal at the tag can fluctuate due to multipath fading and interference, potentially destabilizing the extracted timing reference. To address this, the envelope signal passes through a series capacitor to remove the DC offset before feeding into a ground-referenced comparator, which outputs a square wave independent of amplitude variations, as shown in Fig. 4 (c).

Generating the Sawtooth Reference: The extracted square wave in Fig. 4 (c) lacks the sharp transitions needed for precise sawtooth waveform generation. To address this, it is processed through an RC differentiator circuit followed by a diode (Fig. 4 (d)), producing narrow positive pulses at the rising edges of the square wave. These pulses maintain the exact timing frequency f_{env} of the envelope and serve as precise timing markers for resetting the sawtooth waveform. Since the square wave's amplitude remains unaffected by environmental interference, the extracted pulses are stable

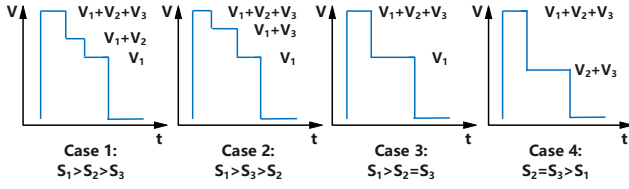| Case 1:
$S_1>S_2>S_3$ | Case 2:
$S_1>S_3>S_2$ | Case 3:
$S_1>S_2=S_3$ | Case 4:
$S_2=S_3>S_1$ |

Figure 5: Voltage-division multiplexing showcase with three sensor streams, ensuring unique and distinguishable summed voltages for each sensor combination.

and consistently trigger an NPN transistor Q_1 to generate the sawtooth waveform (Fig. 4 (e)).

Adapting to Flexible Reference Frequencies: MmBack is designed to interface with a wide range of sensors. Fixed-frequency onboard clocks limit adaptability, as different sensing applications may require varying timing frequencies for optimal performance. For example, biosignal monitoring operates at a few hertz, while ultrasonic tracking requires kilohertz-range frequencies. Adjusting the timing frequency dynamically enhances sensor compatibility while optimizing power consumption by aligning the sampling rate with application requirements. To achieve this, MmBack enables on-the-fly reference frequency tuning without hardware modifications by adjusting a tunable resistor R_{set} on the tag, which regulates the charging current of the sawtooth waveform generator as shown in Fig. 4 (e). We detail the design in Appendix A.

5 VOLTAGE-DIVISION MULTIPLEXING

Once MmBack encodes all sensor inputs into synchronous PWM signals, it must multiplex them onto the backscatter signal. A natural approach might be frequency-division multiplexing, where each sensor stream transmits over a distinct frequency band. However, this requires multiple independent modulation circuits on a single tag, each with its own oscillator and mixer for frequency shifting, significantly increasing power consumption and hardware complexity.

Instead, MmBack introduces a minimalist approach—it sums all synchronous PWM signals into a single voltage signal and processes them through a single modulation chain consisting of just one voltage-controlled oscillators (VCO) and RF switch. A key challenge is ensuring that, even after summation, individual sensor contributions remain uniquely decodable. Rather than naive summation, which can obscure sensor identity due to overlapping voltage levels, MmBack designs a structured voltage-division multiplexing scheme that makes each possible combination of active sensors produce a distinct, decodable voltage sum.

To ensure multiplexed PWM signals remain distinguishable after summation, each sensor signal must contribute a voltage value that allows every unique sensor combination to produce a distinct summed voltage. Fig. 5 shows an example of three sensor streams, where S_1, S_2, S_3 are PWM readings, and V_1, V_2, V_3 represent their assigned voltage contributions. The goal is to construct a composite voltage where any possible subset of sensor contributions—i.e., $[V_1, V_2, V_3, V_1+V_2, V_1+V_3, V_2 + V_3, V_1 + V_2 + V_3]$—remains unique. Even when two sensors have identical readings (e.g., Case 3 and Case 4), the scheme ensures that sensors remain identifiable and their values (i.e., duty cycles) can be accurately recovered.

Design Choice of Voltage Assignment: A potential approach is to assign each sensor stream a unique prime number as its weighted voltage contribution for summation. While this guarantees uniqueness, the sum of prime numbers grows non-linearly. As more sensors are added, the summed voltage values become increasingly large, leading to inefficient use of the available voltage range as more sensors are added.

Instead, MmBack applies a binary-weighted geometric progression for voltage assignment. Specifically, each sensor stream passes through a dedicated resistor before summation, where the resistor values are assigned as:

$$R_i = \alpha R_f \cdot 2^{i-1} \tag{4}$$

where R_i is the resistor value assigned to the ith sensor stream, R_f is the feedback resistor, α is a preset coefficient, i represents the sensor stream index. This configuration assigns each sensor's voltage contribution based on a geometric progression for summation. With this resistor configuration, the summing output voltage V_{out} of all N sensor streams is given by:

$$V_{out} = R_f \sum_{i=1}^{N} \frac{V_s}{R_i} \tag{5}$$

where V_s represents the original voltage level of each sensor's PWM signal, which is the same across all signals. This summation is performed through a proportional summing circuit, which combines the weighted voltage contribution from multiple sensor streams into a single voltage signal, as shown in Fig. 6.

The resistor configuration in Eqn. 4 ensures that every unique combination of sensor streams produces a distinct voltage sum, allowing the receiver to decode and reconstruct individual sensor readings. Furthermore, the geometric progression of resistor values makes uniform voltage spacing between sensor combinations.

Backscatter Modulation of Summed Signal: MmBack modulates the summed voltage signal onto the backscatter carrier by mapping voltage to frequency shifts using a low-power voltage-controlled oscillator (VCO) [12]. The VCO output frequency f_{out} varies linearly between 488 Hz and 1 MHz with the summed voltage V_{out} (detailed in Appendix B). This frequency-modulated signal is then mixed with the 915
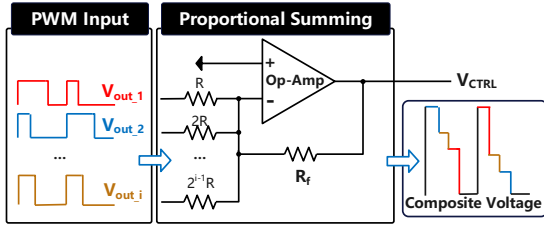
Figure 6: Proportional Summing Circuit.

MHz carrier using an RF switch [11], producing backscatter frequency shifts corresponding to different sensor combinations. In a 5-sensor MMBACK tag, 32 possible sensor combinations are mapped within a 1 MHz bandwidth, resulting in a frequency separation of 31.25 kHz per combination.

6 SIGNAL DEMULTIPLEXING

This section describes how the MMBACK receiver de-multiplexes the backscattered signal into individual sensor readings. Fig. 7(a) shows a spectrogram of the received signal for five sensor streams over three consecutive sampling periods. Each period corresponds to one full cycle of the reference frequency. In this example, the reference frequency is 5 kHz, resulting in a 0.2 ms period. The reference frequency dictates the rate at which sensor signals are sampled and modulated into backscatter frequency shifts.

Within each period, frequency transitions follow a "staircase" pattern, as different sensor combinations produce distinct frequency shifts according to their multiplexed voltage levels. To reconstruct the original sensor readings, MMBACK must 1) segment sampling periods, 2) track frequency levels corresponding to different sensor combinations, 3) and precisely determine the timing of each "staircase" transition. To achieve these, MMBACK must accurately track frequency transitions and determine the precise timing of each shift.

A key challenge is that Discrete Fourier Transform (DFT)-based methods struggle to resolve closely spaced frequency components, causing peak ambiguities in the spectral representation, as shown in Fig. 7(b). This arises due to the fundamental tradeoff between spectral and temporal resolution. Increasing the time window improves frequency resolution, allowing finer separation of spectral peaks. However, a larger time window merges closely spaced frequency transitions, blurring their timing and making it difficult to compute sensor duty cycles. This tradeoff makes it challenging to simultaneously resolve both frequency and timing, which is crucial for demultiplexing the backscatter signal.

Frequency Tracking with Chirp-Z Transform: To address this, MMBACK applies the Chirp-Z Transform (CZT) instead of conventional DFT. Unlike DFT, which uniformly distributes frequency bins, CZT refines bin spacing within a predefined frequency range—specifically, the 1 MHz backscatter bandwidth. This allows MMBACK to densify spectral representation—increasing the frequency bins, without increasing the time window. Fig.7(b) compares CZT with DFT, illustrating CZT's more accurate peak detection.

However, while CZT improves frequency separation, it does not enhance true frequency resolution beyond the limits imposed by the finite window length N, it merely interpolates between existing components for a denser representation. Thus, while CZT resolves spectral ambiguity, it does not improve the timing accuracy of frequency transitions—which is critical for decoding sensor signals.

Tracking Transient Frequency Transitions: To accurately determine transition timing, MMBACK analyzes relative spectral magnitude variations across consecutive CZT windows. As shown in Fig. 7(c), the relative CZT magnitude plot reveals how frequency components evolve during transitions: at each transition, the spectral magnitude of an active frequency gradually fades, while a new frequency component rises. Importantly, the last peak before minimum negative derivative—indicates the exact moment of transition. Thus, MMBACK extracts transition timing through three steps: 1) computes the first derivative of spectral magnitude changes over time; 2) identifies the minimal negative derivative, indicating the steepest falling edge in frequency transition; 3) backtracks to determine the exact start time of each frequency transition. Algorithm 1 details how MM-BACK progressively determines the precise timing of each frequency transition.

Decoding using Finite State Machine: Once frequency shifts and their durations are tracked, the final step is to decode sensor combinations into individual sensor readings. As shown in Fig. 7(a), the frequency follows an ascending staircase pattern within each sampling period. The period always begins with the lowest frequency, corresponding to all active sensors, and steps up as individual sensor signals transition to zero. This structured progression allows us to model the decoding process as a finite-state machine (FSM), which reconstructs sensor combinations over time.

MMBACK leverages two key observations to enhance decoding robustness: 1) State Transitions Follow a Subset Pattern: At each step, the current frequency corresponds to a subset of the previous combination. When a sensor is inactive, the system moves to a new state representing the remaining active sensors. 2) Peak Amplitude Identification: Due to spectral bin correlations in CZT, neighboring frequency bins exhibit high similarity. To accurately identify the active sensor combination at each step, MMBACK selects the frequency with the highest peak, as it contains additional contributions from overlapping spectral components.

(a) Example Backscatter Trace (b) Spectral Analysis (c) Relative CZT
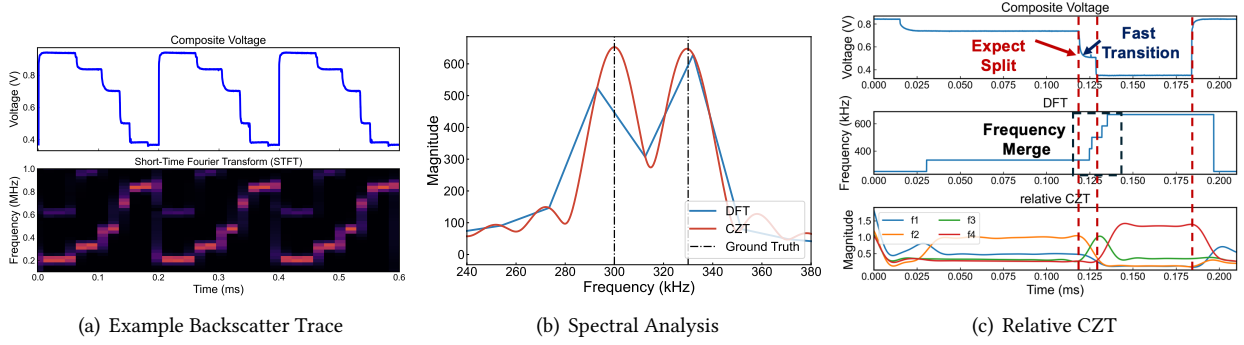
Figure 7: (a) Above: Multiplexed summed voltage signal of five sensor streams with a 5 kHz reference frequency extracted from RF excitation. Below: Spectrogram of the backscattered signal, where frequency transitions indicate different sensor combinations. (b) Frequency tracking comparison: CZT vs. DFT. (c) Relative CZT magnitude tracking frequency transitions, where the minimal negative derivative identifies transition points.

Algorithm 2 details the complete decoding procedure. MM-BACK first identifies period boundaries by detecting the transition to the lowest frequency state, where no sensors are active. Within each period, it obtains frequency traces using CZT and use Algo.1 to detect the timing of transient frequency shifts. Starting from the lowest frequency state, it traces backward, selecting the dominant frequency levels using FSM. The FSM outputs the correct sequence of sensor combinations and their corresponding time durations, which are then used to reconstruct individual sensor readings based on PWM duty cycles.

7 IMPLEMENTATION

At the heart of MMBACK is a novel backscatter tag that enables synchronous sensor readings and multiplexing from multiple sensors without requiring an onboard clock. The key enablers are two low-power modules: 1) a timing extraction module that enables clock-free, synchronized sensor acquisition, and 2) a voltage-division multiplexing module that efficiently encodes multiple PWM signals.

Timing Extraction Module: This module (see Fig. 8 (a.1)) includes two key components: (1) a parallel architecture that reads multiple sensor inputs concurrently; (2) a sawtooth reference signal generation circuit that derives a shared timing reference from the ambient RF excitation and generates sawtooth waveforms. Together, these components avoid the use of an onboard clock while ensuring simultaneous and synchronous readings across multiple sensors.

1) Parallel Architecture: MMBACK synchronizes sensor readings by comparing all sensor inputs against a shared sawtooth reference. To support plug-and-play sensor modules (typically outputting 0–3.3V), it uses parallel micro-power comparators (TLV3201 [24]) operating at 3.3V. These comparators provide low propagation delay ($<40ns$) with minimal

skew ($<2ns$) for precise synchronization. A 6-way switch in our prototype configures the number of sensors. Each sensor input is converted into a 3.3V PWM signal.

2) Sawtooth Reference generation: MMBACK generates a sawtooth reference for PWM encoding by extracting a frequency reference using an envelope detector with a four-stage Schottky diode rectifier (HSMS285C) and a 100 kHz low-pass filter to remove unintended high-tone components. To mitigate interference, a micropower comparator (LTC6702) converts the filtered envelope into a square wave, which then passes through an RC differentiator and diode (1N4148) to produce positive pulses at each rising edge. These pulses trigger an NPN transistor (1N5551) that controls the charging of a 500 pF capacitor via a constant current source. The current source, implemented with a zener diode (BZT52C3V3) and a PNP transistor (2N5401), maintains a regulated 3.3V output. A potentiometer ($20-200\ k\Omega$) adjusts the charging current, allowing flexible frequency tuning while keeping the peak output voltage constant at 3.3V.

Multiplexing Module: This module (see Fig. 8 (a.2&a.3)) multiplexes synchronous PWM signals using a novel voltage-division multiplexing scheme, which sums all signals into a single composite voltage while ensuring they remain uniquely decodable, as described in Sec. 5. A low-power operational amplifier (AD8605) forms a proportional summing circuit, generating a stepwise voltage signal that is scaled below 1V before being fed into the backscatter front-end.

Backscatter Front-end: The backscatter modulation of MMBACK tag is based on the architecture proposed in [40]. The multiplexed summed voltage is converted to frequency shifts via a VCO (LTC6990) and modulated onto the carrier wave using an RF switch (ADG902). Specifically, the VCO

maps voltage variations from 0V to 1V into frequency shifts ranging from 1 MHz to 100 kHz.

IC Design: We design ASIC of MMBACK using Cadence IC6.17 Virtuso. The design is implemented in the Virtuso analog design environment using the TSMC 65nm CMOS Low Power technology library. The ASIC design shows that the overall power consumption for timing reference extraction and signal multiplexing is 7.47 μW and 18.09 μW, respectively. The power consumption of each component's prototype is described in Sec. 8.4.

8 EVALUATION

8.1 Evaluation Methodology

MMBACK Tag: We implemented our MMBACK prototype using purely off-the-shelf analog components to ensure low-power consumptions. For experiments, we used a six-way switch to flexibly control the number of channels. As shown in Fig. 8(b), MMBACK uses two common low-cost 915 MHz antennas, each with a 3 dBi gain, for sawtooth reference signal generation and backscatter circuits. The overall cost of MMBACK is around 17 USD. With a preliminary two-layer PCB prototype, power consumption varies between $1.36mW \sim 2.32mW$, depending on the number of sensors (1 to 5) and reference frequencies. The tag can achieve a more compact form factor of $32mm \times 25mm$ if remove the switch, as shown in Fig. 8(a).

MMBACK Station: We use a USRP B210 connected to an amplifier as a 915MHz RF transmitter module that sends a double-tone carrier signal. The transmission power is of 20 dBm and transmitted through a 9 dBi polarized antenna. On the receiver side, we used a USRP N210 software-defined radio (SDR) equipped with an SBX-40 daughterboard [17], which supports a 20 MHz sampling rate. The backscatter signal is captured using a 9 dBi polarized antenna.

MMBACK Software: All software processing takes place within the MMBACK station. The RF signal is continuously decoded into multi-channel sensor signals on a 2023 Mac-Book Pro, with the decoding algorithm entirely implemented in Python.

Ground truth: Commercial sensor modules typically output a continuous voltage in the range of 0 to 3.3V. In our evaluation, we use a signal generator to flexibly adjust the input voltage, simulating sensor readings to effectively evaluate the performance of MMBACK. Note that in the application phase, we will use real sensors to collect signals.

Environments: The experiments were conducted in an indoor environment consisting of multiple rooms furnished with tables and chairs, as shown in the floor plan (Fig. 8 (c)). We performed tests under both line-of-sight (LOS) and non-line-of-sight (NLOS) conditions.

Evaluation metrics: We use Signal-to-Noise Ratio (SNR) to evaluate the signal recovery quality, representing the distortion to the desired signal. The SNR between an input signal from generator $x \in R^{1 \times T}$ and the decoded RF signal $\hat{x} \in R^{1 \times T}$ is defined as : $SNR(x, \hat{x}) = 10 \log_{10} \left(\frac{||x||_2^2}{||x - \hat{x}||_2^2} \right)$. For evaluation, we sample ten different data sequences and report the average SNR among all the sensors.

8.2 Overall Performance

In this section, we evaluate the impact of overall performance. We used a USRP N210 to sample the RF signal at 20 MHz. Without special instructions, the default settings of MMBACK is listed as following: the excitation-to-tag distance and the tag-to-reader distance is set $1m$ and $5m$, respectively. The channel number is 3 or 5, and the input signal is a 1kHz single-tone signal with random phase and amplitude. We take the average SNR of all sensors as the evaluation metrics.

8.2.1 Reference frequency. The reference frequency, derived from the RF excitation source, dictates the rate at which sensor signals are sampled. It defines the duration of each sampling period, influencing both the timing resolution and the complexity of the decoding process. With a fixed receiver sampling rate, increasing the reference frequency shortens each sampling period, reducing the number of data samples available per period. This presents challenges for the decoding algorithm, as fewer samples make it harder to accurately reconstruct sensor signals. We evaluate the impact of reference frequency.

Method: We evaluate MMBACK's SNR with three streams up to 50 kHz and five streams up to 20 kHz.

Results: Fig. 9(a) shows the SNR for 3-streams, peaking at a $10kHz$ reference frequency. This outperforms $5kHz$ since higher reference frequency sample more signal details, enhancing overall signal quality. However, increasing the reference frequency also complicates demultiplexing, leading to slight performance degradation. As shown in Fig. 9, MMBACK supports up to $50kHz$ with $15dB$ SNR for 3 streams, while Fig.9(b) shows that it supports up to $20kHz$ kHz with $15dB$ SNR for five sensor streams.

8.2.2 Tag-to-Rx distance. In this section, we evaluate the impact of the tag-to-receiver distance.

Method: We placed the MMBACK tag close to the excitation source. We initially place the reader at a distance of $2m$ to the tag. Then we move the reader to increase the distance between MMBACK and the reader from $2m$ to $12m$. We measure the SNR changes 5 times on sampling a $1kHz$ signal with $10kHz$ reference frequency, each time with random amplitude and phase. We did the experiments twice, once on the LOS path and another on the NLOS path.
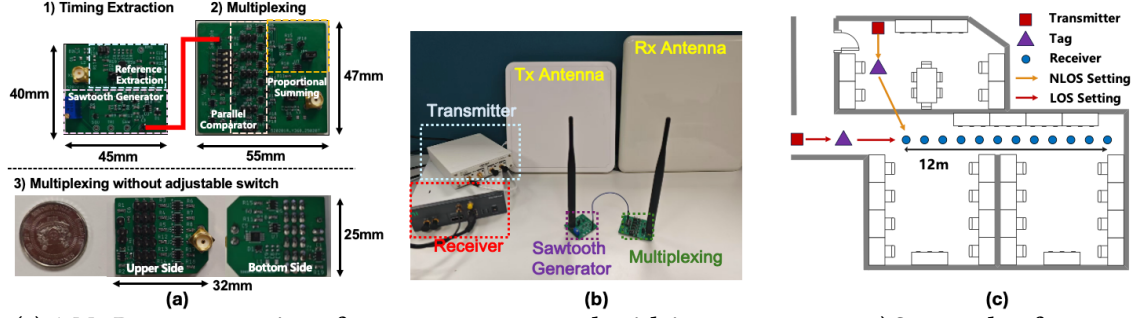
Figure 8: (a) A MMBACK tag consists of two components, each with its own antenna: 1) Sawtooth reference generation, which extracts timing signals from ambient RF excitation, and 2) Signal multiplexing and backscatter transmission. These two components are wired together using a jumper wire. (b) Experiment setup. (c) Floorplan.
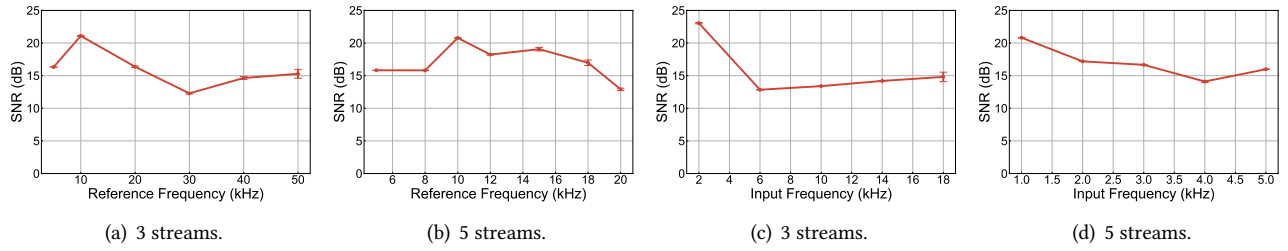

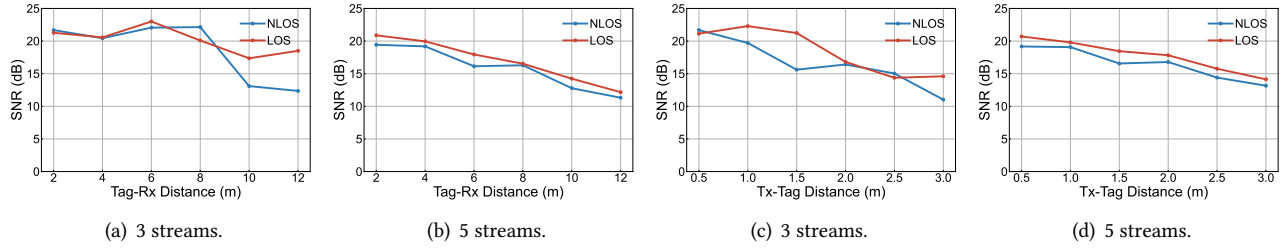Figure 9: (a&b) SNR variation with reference frequency. (c&d) SNR variation with sensor input frequency.

Figure 10: (a&b) SNR under impact of Tag-to-Rx distance. (c&d) SNR under impact of Tag-to-Tx distance.

Results: Fig. 10 (a&b) shows the results that for both 3 streams and 5 streams condition, MMBACK can both achieve over 12 dB signal reconstruction. In the NLOS situation, there will be a sudden drop when moving to 10m, while it was relatively stable before. The reason is that MMBACK based on frequency-tracking approach, which is not particularly sensitive to abosolute signal strength.

8.2.3 Tx-to-Tag distance. Then we examine how the Tx-to-tag distance impacts the signal recovering quality.
Method: Here we place the reader with a fixed distance of 2m away from the MMBACK tag. Then we increase the excitation distance from 0.5m to 3m and measure the SNR changes under different reference frequencies. We also did the experiments on both LOS and NLOS scenarios.
Results: As shown in Fig. 10 (c&d), from 0.5m to 3m, the quality of signal reconstruction drops from 20dB to 10dB.

The performance under LOS condition is always better than that of NLOS condition, whether it is 3 streams or 5 streams.

8.2.4 Inter-sensor delays. One typical advantages of MM-BACK is that the sensor signal of each channel is sample synchronously. We use a signal generator to input the same sine wave signal to each sensor branch, and then use an oscilloscope to see whether the resulting composite signal will form multiple steps. If the signals are not synchronized, multiple steps will be generated on the composite voltage. If the signals are synchronized, there will only be one falling edge. Our oscilloscope has a sampling rate of 100MHz, and we can see a difference of more than 10ns. However, we only saw one falling edge, which indicates that the inter-sensor delay is less than 10 ns.
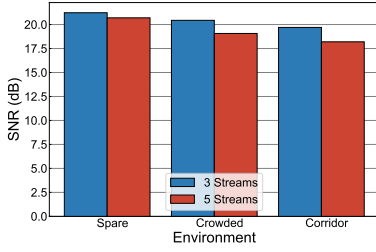
Figure 11: Impact of environmental interference.

Table 2: Power consumption of MмBacк in both PCB and ASIC design.

	Sawtooth Generator			Multiplexing	
Freq	PCB	IC	Num.	PCB	IC
5kHz	191.26μW	7.375 μW	1	1.14 mW	10.68 μW
10kHz	230.26μW	7.423 μW	2	1.29 mW	12.77 μW
20kHz	312.49μW	7.454 μW	3	1.45 mW	14.76 μW
30kHz	394.35μW	7.463 μW	4	1.60 mW	16.59 μW
40kHz	466.81μW	7.467 μW	5	1.78 mW	18.09 μW
50kHz	542.51μW	7.47 μW			

8.3 Impact of Factors

8.3.1 Input signal frequency. The frequency of the sensor readings may cover a wide range. In this section, we evaluate the impact of the input signal frequency.

Methods: We did the evaluation with 5 sensor channels. We input signal ranging from $2kHz$ to $18kHz$ and $1kHz$ to $5kHz$ for 3 streams and 5 streams, respectively. The reference frequency is set larger than double Nyquist frequency. We evaluate the SNR of the recovered signal.

Results: Fig.9 (c&d) show that the performance all exceed $20dB$ SNR at the beginning. As the frequency increases, the performance begins to decrease, but it always remains at a good level (i.e., $15dB$ SNR). This means that MмBacк can perform well when the Nyquist sampling rate is met.

8.3.2 Environmental Interference. The movement of people in the environment can have a real-time impact on signal strength. The multi-path fading may also influence the signal propagation.

Method: To account for this, we evaluated MмBacк in different scenarios: a spacious indoor room, a crowded room furnished with tables and chairs, and a frequently used corridor that is intermittently obstructed by passersby.

Results: As can be seen from Fig. 11, the SNR under 3 streams is always better than that under 5 streams. In a spare environment, the SNR is higher, while in crowded environment, SNR is relatively lower. Nevertheless, the SNR all exceeded 15 dB, which indicates that MмBacк can work well in various environments.
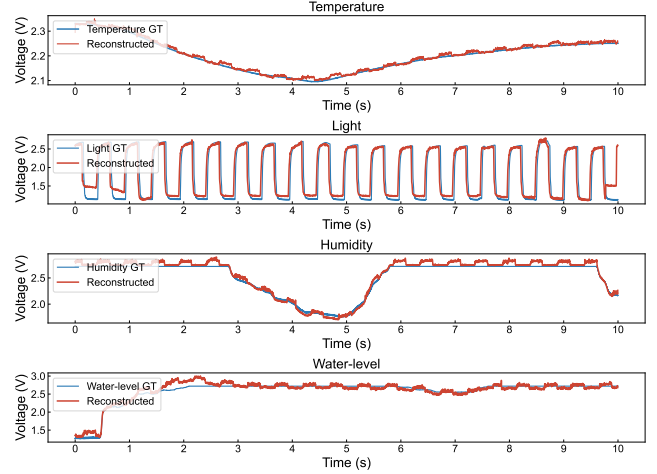

Figure 12: Plant sensing with four sensors.

8.4 Power consumption

In this section, we evaluate the power consumption of Mм-Bacк tag. The tag consists two majority functionalities: sawtooth generator, multiplexing and backscatter circuit. Table. 2 shows the detailed power consumption of each part under different reference frequency and different number of sensor streams. The PCB implementation of sawtooth generator consumes 191.26μW to 542.51μW for generating 3.3V sawtooth reference from $5kHz$ to $50kHz$. As for multiplexing circuit, it consumes 1.14mW to 1.78mW from 1 sensor stream to 5 sensor streams. Each comparator consumes 127μW for each branch. The most energy consuming part is the operational amplifier with the proportional resistance, which consumes above 600μW, accounts for > 30%. The LTC6990 VCO typically consumes 320μW to backscatter frequency shift on the carriers.

We also optimize the power consumption in the ASIC simulation. The ASIC design shows that the the sawtooth generator part typically consumes 7.47μW for generating 50 kHz reference frequency. For the multiplexing, ASIC design consumes 10.68μW to 18.09μW accounting for 1 to 5 sensors. Therefore, the total consumption of MмBacк tag in ASIC design is 25.56μW for 5 sensor streams under $50kHz$ reference frequency.

8.5 Application Use Cases

MмBacк is a general-purpose interface that supports multiple sensors. In this section, we showcase three representative applications of MмBacк including plant sensing, acoustic AoA tracking, and human health monitoring, including 9 different off-the-shelf sensors. The sensor models used are listed in Appendix D.

8.5.1 Plant Sensing. Plant healthcare monitoring systems [32] often require concurrent streaming from multiple types of sensors. We implemented the MMBACK tag for plant monitoring by interfacing with off-the-shelf sensors, including a temperature sensor, an optical sensor, a soil moisture sensor, and a water-level sensor. We verified MMBACK 's functionality by adjusting the temperature, flickering the lights, contacting moisture sensors with moist soil, and placing water level gauges at different depths. A synchronous ADC was used as the ground truth for data sampling, and we recovered the signal from the backscatter transmission for comparison. Fig. 12 shows the ground truth and the reconstructed results, demonstrating that the restored signal closely matches the ground truth. The pulse-like disturbances result from the optical sensor's rapid amplitude changes, which introduce slight interference in the demultiplexing process.

8.5.2 Acoustic AoA estimation. Microphone arrays are commonly used for acoustic tracking based on angle-of-arrival (AoA) estimation. We conduct experiments using four identical microphones, interfaced with MMBACK. We played a single-tone wave at 1 kHz and 5 kHz from different angles using a loudspeaker, while MMBACK simultaneously captured signals from all microphones. Our results show that the estimated Angle-of-Arrival error is 3.6° for the 1 kHz wave and 11.7° for the 5 kHz wave.

8.5.3 Human health monitoring. Backscatter-based wearable devices can integrate a variety of sensors to monitor human health. We demonstrate MMBACK 's capability by integrating four physiological sensors: a respiration sensor, a PPG sensor, an ECG sensor, and an arterial blood pressure (ABP) sensor. Unlike plant sensing, where changes occur gradually, physiological signals exhibit periodicity and short pulses. Accurate pulse tracking is crucial for health applications such as blood pressure monitoring, which relies on estimating pulse transit time (PTT) [47] by measuring the time difference between ECG and PPG pulse waveforms. Fig. 13 shows the signal reconstruction from 4 sensor streams. The results indicate that MMBACK effectively captures short-duration pulse signals and reconstructs sensor readings.

9 DISCUSSION AND LIMITATIONS

Number of Sensors Per Tag: The current prototype of MMBACK supports up to five sensors per tag, with potential for further scalability. The primary constraint on the number of sensor streams per MMBACK tag is the VCO's 1 MHz frequency shift range [12]. As more sensors are added, the differences between distinct summed voltages decrease, reducing the separation between their corresponding frequency shifts. To ensure reliable signal recovery, MMBACK
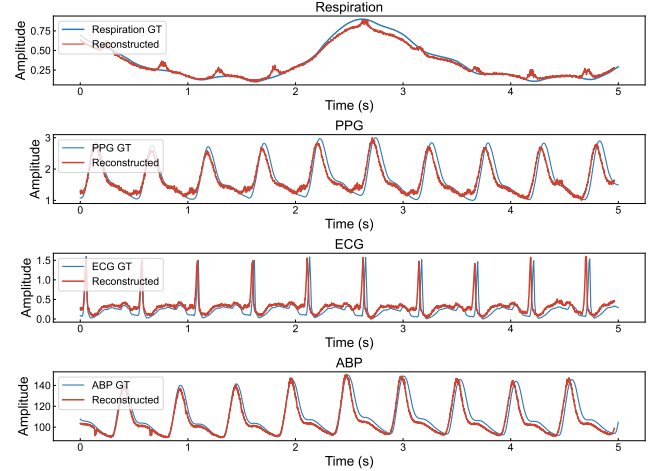

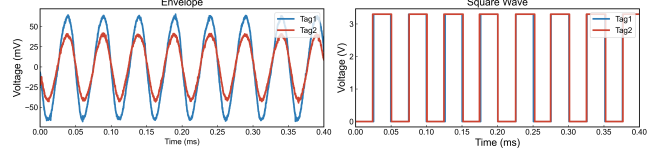Figure 13: Human health monitoring with four sensors

Figure 14: Precise Synchronization between Tags.

conservatively sets the frequency shift spacing to 31.25 kHz for five sensors.

Multi-tag Scenario: For deployments requiring monitoring multiple subjects in the same environment (e.g., individuals in a smart home setting), MMBACK can be extended by incorporating a low-power state machine [69] to implement anti-collision protocols, similar to RFID's slotted ALOHA protocol. This enables multiple MMBACK tags to coexist without interference, allowing tracking of multiple subjects. Additionally, since all sensors on the MMBACK tag share the same antenna for backscattering—typically the largest physical component in tags—it offers a more compact alternative to single-sensor-per-tag designs.

Power Consumption: While ASIC simulations show that MMBACK's IC design consumes only 25.56 μW, our preliminary PCB implementation currently operates at 2.1 mW. A major constraint arises from the plug-and-play sensor modules (e.g., sensors sold by Adafruit, SparkFun) used in our experiments, which often require higher supply voltages (e.g., 3.3V) for compatibility. However, for specialized or MEMS-based sensors with lower voltage requirements, MM-BACK could reduce its supply voltage further, significantly lowering overall power consumption. Moreover, additional energy-harvesting sources (e.g., solar [37] or acoustic [3, 36]) along with intermittent operation via a supercapacitor [43] could facilitate fully battery-free operation of MMBACK.

Synchronization between tags: MMBACK extracts its timing frequency from the RF excitation source, enabling multiple tags in the same space to share a common reference

frequency for natural synchronization among tags. Fig. 14 shows this with two tags placed $1m$ apart. We measured the envelope and the produced square wave. The results show that though the envelope amplitude varies, the amplitudes of resulting square waves remain consistent, which support to generate consistent sawtooth. The slight timing differences stem from time-of-flight delays at the nanosecond level, which are negligible for kHz sensing applications. This highlights MMBACK's potential for globally synchronized deployments across multiple objects.

10 CONCLUSION

This paper presents MMBACK, a clock-free backscatter sensor interface that enables synchronous multi-sensor data acquisition and multiplexing via a single modulation chain. By extracting a shared sawtooth reference from ambient RF excitation, MMBACK eliminates the need for onboard clocks, ensuring precise synchronization across sensor streams. We further design a voltage-division scheme to multiplex sensor signals as backscatter frequency shifts using a single modulation chain. We then develop frequency tracking algorithms based on consecutive spectral magnitude variations and FSM for demultiplexing. We demonstrate that MMBACK supports three concurrent sensors with bandwidths up to 18 kHz, and five concurrent sensors with bandwidths up to 5 kHz with applications in health monitoring and AoA estimation.

REFERENCES

[1] Ali Abedi, Farzan Dehbashi, Mohammad Hossein Mazaheri, Omid Abari, and Tim Brecht. Witag: Seamless wifi backscatter communication. In *Proceedings of the Annual conference of the ACM Special Interest Group on Data Communication on the applications, technologies, architectures, and protocols for computer communication*, pages 240–252, 2020.

[2] Adafruit Industries LLC. 4965 - stemma soil sensor - i2c capacitive moisture sensor. https://www.digikey.sg/en/products/detail/adafruit-industries-llc/4965/14302510. Accessed: 2025-03-19.

[3] Sayed Saad Afzal, Waleed Akbar, Osvy Rodriguez, Mario Doumet, Unsoo Ha, Reza Ghaffarivardavagh, and Fadel Adib. Battery-free wireless imaging of underwater environments. *Nature Communications*, 13:5546, 2022.

[4] Mervin Chun-Yi Ang, Jolly Madathiparambil Saju, Thomas K Porter, Sayyid Mohaideen, Sreelatha Sarangapani, Duc Thinh Khong, Song Wang, Jianqiao Cui, Suh In Loh, Gajendra Pratap Singh, et al. Decoding early stress signaling waves in living plants using nanosensor multiplexing. *Nature Communications*, 15(1):2943, 2024.

[5] Arduino. Arduino sensor kit - bundle. https://store.arduino.cc/collections/kits/products/arduino-sensor-kit-bundle. Accessed: 2025-03-19.

[6] Nagarjun Bhat, Agrim Gupta, Ishan Bansal, Harine Govindarajan, and Dinesh Bharadia. Zensetag: An rfid assisted twin-tag single antenna cots sensor interface. In *Proceedings of the 22nd ACM Conference on Embedded Networked Sensor Systems*, pages 336–350, 2024.

[7] Liqiong Chang, Jie Xiong, Ju Wang, Xiaojiang Chen, Yu Wang, Zhanyong Tang, and Dingyi Fang. Rf-copybook: A millimeter level calligraphy copybook based on commodity rfid. *Proc. ACM Interact. Mob.*

Wearable Ubiquitous Technol., 1(4), January 2018.

[8] Li-Xuan Chuo, Zhihong Luo, Dennis Sylvester, David Blaauw, and Hun-Seok Kim. Rf-echo: A non-line-of-sight indoor localization system using a low-power active rf reflector asic tag. In *Proceedings of the 23rd Annual International Conference on Mobile Computing and Networking*, MobiCom '17, page 222–234, New York, NY, USA, 2017. Association for Computing Machinery.

[9] Tuan Dang, Trung Tran, Khang Nguyen, Tien Pham, Nhat Pham, Tam Vu, and Phuc Nguyen. iotree: a battery-free wearable system with biocompatible sensors for continuous tree health monitoring. In *Proceedings of the 28th Annual International Conference on Mobile Computing And Networking*, pages 352–366, 2022.

[10] Analog Devices. The abcs of analog to digital converters: How adc errors affect system performance. https://www.analog.com/en/resources/technical-articles/the-abcs-of-analog-to-digital-converters-how-adc-errors-affect-system-performance.html?utm_source=chatgpt.com, 2002.

[11] Analog devices. Adg901/adg902, 0 hz to 4.5 ghz, 40 db off isolation at 1 ghz, 17 dbm p1db at 1 ghz spst switches. https://www.analog.com/media/en/technical-documentation/data-sheets/ADG901_902.pdf, 2024.

[12] Analog devices. Timerblox: Voltage controlled silicon oscillator, ltc6990. https://www.analog.com/media/en/technical-documentation/data-sheets/ltc6990.pdf, 2024.

[13] DFRobot. Moisture sensor (sku: Sen0114). https://wiki.dfrobot.com/Moisture_Sensor__SKU_SEN0114_. Accessed: 2025-03-19.

[14] DFRobot. Sen0203 - gravity: Analog capacitive soil moisture sensor. https://www.digikey.sg/en/products/detail/dfrobot/SEN0203/6588613. Accessed: 2025-03-19.

[15] DFRobot. Sen0213 - analog heart rate monitor sensor. https://sg.element14.com/dfrobot/sen0213/analog-heart-rate-monitor-sensor/dp/2946130. Accessed: 2025-03-19.

[16] Digikey. Xc3s500e-4pq208i. https://www.digikey.com/en/products/detail/amd/XC3S500E-4PQ208I/2500930, 2024.

[17] DIGILENT. Sbx 400-4400 mhz for ettus usrp n210: Rx/tx (40 mhz). https://digilent.com/shop/sbx-400-4400-mhz-for-ettus-usrp-n210-rx-tx-40-mhz/?srsltid=AfmBOooCKkLCEaGM6pj3Ytn1JBPLfE2FJXAPxYKvEf-q345df4wsqvZI, 2024.

[18] Shuya Ding, Zhe Chen, Tianyue Zheng, and Jun Luo. Rf-net: A unified meta-learning framework for rf-enabled one-shot human activity recognition. In *Proceedings of the 18th Conference on Embedded Networked Sensor Systems*, pages 517–530, 2020.

[19] Chuhan Gao, Yilong Li, and Xinyu Zhang. LiveTag: Sensing Human-Object interaction through passive chipless WiFi tags. In *15th USENIX Symposium on Networked Systems Design and Implementation (NSDI 18)*, pages 533–546, Renton, WA, April 2018. USENIX Association.

[20] Guorong He, Yaxiong Xie, Chao Zheng, Longlong Zhang, Qi Wu, Wenyan Zhang, Dan Xu, and Xiaojiang Chen. Hornbill: A portable, touchless, and battery-free electrochemical bio-tag for multi-pesticide detection. In *Proceedings of the 30th Annual International Conference on Mobile Computing and Networking*, pages 1283–1298, 2024.

[21] Elisabeth Ilie-Zudor, Zsolt Kemény, Fred Van Blommestein, László Monostori, and André Van Der Meulen. A survey of applications and requirements of unique identification systems and rfid techniques. *Computers in Industry*, 62(3):227–252, 2011.

[22] Texas Instruments. Adc accuracy: Effect of temperature drift on adc signal chain (part 3). https://e2e.ti.com/blogs_/archives/b/precisionhub/posts/adc-accuracy-effect-of-temperature-drift-on-adc-signal-chain-part-3?utm_source=chatgpt.com, 2015.

[23] Texas Instruments. Design for msp430fr4xx and msp430fr2xx. https://www.ti.com.cn/cn/lit/an/zhca984a/zhca984a.pdf?utm_source=chatgpt.com&ts=1740300023359&ref_url=https%253A%252F%252Fchatgpt.com%252F, 2024.

[24] Texas Instruments. Tlv320x 40ns, micropower, push-pull output comparators. https://www.ti.com/lit/ds/symlink/tlv3201.pdf?ts=1742257477890&ref_url=https%253A%252F%252Fwww.ti.com.cn%252Fproduct%252Fcn%252FTLV3201, 2024.

[25] Sijie Ji, Xuanye Zhang, Yuanqing Zheng, and Mo Li. Construct 3d hand skeleton with commercial wifi. In *Proceedings of the 21st ACM Conference on Embedded Networked Sensor Systems*, SenSys '23, page 322–334, New York, NY, USA, 2024. Association for Computing Machinery.

[26] Subhajit Karmakar, Atsutse Kludze, and Yasaman Ghasempour. Metasticker: Sub-terahertz metamaterial stickers for non-invasive mobile food sensing. In *Proceedings of the 21st ACM Conference on Embedded Networked Sensor Systems*, SenSys '23, page 335–348, New York, NY, USA, 2024. Association for Computing Machinery.

[27] Bryce Kellogg, Vamsi Talla, and Shyamnath Gollakota. Bringing gesture recognition to all devices. In *11th USENIX Symposium on Networked Systems Design and Implementation (NSDI 14)*, pages 303–316, Seattle, WA, April 2014. USENIX Association.

[28] Usman Mahmood Khan and Muhammad Shahzad. Estimating soil moisture using rf signals. In *Proceedings of the 28th Annual International Conference on Mobile Computing And Networking*, MobiCom '22, page 242–254, New York, NY, USA, 2022. Association for Computing Machinery.

[29] Gierad Laput, Yang Zhang, and Chris Harrison. Synthetic sensors: Towards general-purpose sensing. In *Proceedings of the 2017 CHI Conference on Human Factors in Computing Systems*, pages 3986–3999, 2017.

[30] Giwon Lee, Oindrila Hossain, Sina Jamalzadegan, Yuxuan Liu, Hongyu Wang, Amanda C Saville, Tatsiana Shymanovich, Rajesh Paul, Dorith Rotenberg, Anna E Whitfield, et al. Abaxial leaf surface-mounted multimodal wearable sensor for continuous plant physiology monitoring. *Science Advances*, 9(15):eade2232, 2023.

[31] Dong Li, Shirui Cao, Sunghoon Ivan Lee, and Jie Xiong. Experience: practical problems for acoustic sensing. In *Proceedings of the 28th Annual International Conference on Mobile Computing And Networking*, pages 381–390, 2022.

[32] Yuyao Lu, Kaichen Xu, Lishu Zhang, Minako Deguchi, Hiroaki Shishido, Takayuki Arie, Ruihua Pan, Akitoshi Hayashi, Lei Shen, Seiji Akita, et al. Multimodal plant healthcare flexible sensor system. *ACS nano*, 14(9):10966–10975, 2020.

[33] Soumyajit Mandal, Lorenzo Turicchia, and Rahul Sarpeshkar. A low-power, battery-free tag for body sensor networks. *IEEE Pervasive Computing*, 9(1):71–77, 2010.

[34] Metrodyne Microsystems. Mps20n0040d-s pressure sensor datasheet. https://softroboticstoolkit.com/files/sorotoolkit/files/mps20n0040d-s_datasheet.pdf. Accessed: 2025-03-19.

[35] Xin Na, Xiuzhen Guo, Zihao Yu, Jia Zhang, Yuan He, and Yunhao Liu. Leggiero: Analog wifi backscatter with payload transparency. In *Proceedings of the 21st Annual International Conference on Mobile Systems, Applications and Services*, MobiSys '23, page 436–449, New York, NY, USA, 2023. Association for Computing Machinery.

[36] Nazish Naeem, Jack Rademacher, Ritik Patnaik, Tara Boroushaki, and Fadel Adib. Seascan: An energy-efficient underwater camera for wireless 3d color imaging. In *Proceedings of the 30th Annual International Conference on Mobile Computing and Networking*, ACM MobiCom '24, page 785–799, New York, NY, USA, 2024. Association for Computing Machinery.

[37] Aaron N. Parks, Angli Liu, Shyamnath Gollakota, and Joshua R. Smith. Turbocharging ambient backscatter communication. In *Proceedings of the 2014 ACM Conference on SIGCOMM*, SIGCOMM '14, page 619–630, New York, NY, USA, 2014. Association for Computing Machinery.

[38] Radislav A. Potyrailo and Cheryl Surman. A passive radio-frequency identification (rfid) gas sensor with self-correction against fluctuations of ambient temperature. *Sensors and Actuators B: Chemical*, 185:587–593, 2013.

[39] Swadhin Pradhan and Lili Qiu. Rtsense: passive rfid based temperature sensing. In *Proceedings of the 18th Conference on Embedded Networked Sensor Systems*, SenSys '20, page 42–55, New York, NY, USA, 2020. Association for Computing Machinery.

[40] Vaishnavi Ranganathan, Sidhant Gupta, Jonathan Lester, Joshua R Smith, and Desney Tan. Rf bandaid: A fully-analog and passive wireless interface for wearable sensors. *Proceedings of the ACM on Interactive, Mobile, Wearable and Ubiquitous Technologies*, 2(2):1–21, 2018.

[41] Ill-Keun Rhee, Jaehan Lee, Jangsub Kim, Erchin Serpedin, and Yik-Chung Wu. Clock synchronization in wireless sensor networks: An overview. *Sensors*, 9(1):56–85, 2009.

[42] Chris M Roberts. Radio frequency identification (rfid). *Computers & security*, 25(1):18–26, 2006.

[43] Alanson P. Sample, Daniel J. Yeager, Pauline S. Powledge, Alexander V. Mamishev, and Joshua R. Smith. Design of an rfid-based battery-free programmable sensing platform. *IEEE Transactions on Instrumentation and Measurement*, 57(11):2608–2615, 2008.

[44] Taweesak Sanpechuda and La-or Kovavisaruch. A review of rfid localization: Applications and techniques. In *2008 5th international conference on electrical engineering/electronics, computer, telecommunications and information technology*, volume 2, pages 769–772. IEEE, 2008.

[45] Sensirion AG. Sfm3020 digital flow sensor product page. https://sensirion.com/products/catalog/SFM3020. Accessed: 2025-03-19.

[46] Longfei Shangguan, Zimu Zhou, and Kyle Jamieson. Enabling gesture-based interactions with objects. In *Proceedings of the 15th Annual International Conference on Mobile Systems, Applications, and Services*, MobiSys '17, page 239–251, New York, NY, USA, 2017. Association for Computing Machinery.

[47] Revati Shriram, Asmita Wakankar, Nivedita Daimiwal, and Dipali Ramdasi. Continuous cuffless blood pressure monitoring based on ptt. In *2010 International Conference on Bioinformatics and Biomedical Technology*, pages 51–55. IEEE, 2010.

[48] Jian Su, Alex X Liu, Zhengguo Sheng, and Yongrui Chen. A partitioning approach to rfid identification. *IEEE/ACM Transactions on Networking*, 28(5):2160–2173, 2020.

[49] Xue Sun, Jie Xiong, Chao Feng, Xiaohui Li, Jiayi Zhang, Binghao Li, Dingyi Fang, and Xiaojiang Chen. Gastag: A gas sensing paradigm using graphene-based tags. In *Proceedings of the 30th Annual International Conference on Mobile Computing and Networking*, pages 342–356, 2024.

[50] Zehua Sun, Tao Ni, Yongliang Chen, Di Duan, Kai Liu, and Weitao Xu. Rf-egg: An rf solution for fine-grained multi-target and multi-task egg incubation sensing. In *Proceedings of the 30th Annual International Conference on Mobile Computing and Networking*, ACM MobiCom '24, page 528–542, New York, NY, USA, 2024. Association for Computing Machinery.

[51] Anran Wang and Shyamnath Gollakota. Millisonic: Pushing the limits of acoustic motion tracking. In *Proceedings of the 2019 CHI conference on human factors in computing systems*, pages 1–11, 2019.

[52] Jingxian Wang, Chengfeng Pan, Haojian Jin, Vaibhav Singh, Yash Jain, Jason I. Hong, Carmel Majidi, and Swarun Kumar. Rfid tattoo: A wireless platform for speech recognition. *Proc. ACM Interact. Mob. Wearable Ubiquitous Technol.*, 3(4), September 2020.

[53] Jingxian Wang, Vaishnavi Ranganathan, Jonathan Lester, and Swarun Kumar. Ultra low-latency backscatter for fast-moving location tracking.

Proceedings of the ACM on Interactive, Mobile, Wearable and Ubiquitous Technologies, 6(1):1–22, 2022.

[54] Ju Wang, Omid Abari, and Srinivasan Keshav. Challenge: Rfid hacking for fun and profit. In *Proceedings of the 24th Annual International Conference on Mobile Computing and Networking*, pages 461–470, 2018.

[55] Ju Wang, Liqiong Chang, Shourya Aggarwal, Omid Abari, and Srinivasan Keshav. Soil moisture sensing with commodity rfid systems. In *Proceedings of the 18th International Conference on Mobile Systems, Applications, and Services*, MobiSys '20, page 273–285, New York, NY, USA, 2020. Association for Computing Machinery.

[56] Ju Wang, Jie Xiong, Xiaojiang Chen, Hongbo Jiang, Rajesh Krishna Balan, and Dingyi Fang. Tagscan: Simultaneous target imaging and material identification with commodity rfid devices. In *Proceedings of the 23rd Annual International Conference on Mobile Computing and Networking*, MobiCom '17, page 288–300, New York, NY, USA, 2017. Association for Computing Machinery.

[57] Ju Wang, Jie Xiong, Hongbo Jiang, Xiaojiang Chen, and Dingyi Fang. D-watch: Embracing "bad" multipaths for device-free localization with cots rfid devices. *IEEE/ACM Transactions on Networking*, 25(6):3559–3572, 2017.

[58] Jue Wang and Dina Katabi. Dude, where's my card? rfid positioning that works with multipath and non-line of sight. In *Proceedings of the ACM SIGCOMM 2013 Conference on SIGCOMM*, SIGCOMM '13, page 51–62, New York, NY, USA, 2013. Association for Computing Machinery.

[59] Juexing Wang, Yuda Feng, Gouree Kumbhar, Guangjing Wang, Qiben Yan, Qingxu Jin, Robert C Ferrier, Jie Xiong, and Tianxing Li. Soilcares: Towards low-cost soil macronutrients and moisture monitoring using rf-vnir sensing. In *Proceedings of the 22nd Annual International Conference on Mobile Systems, Applications and Services*, pages 196–209, 2024.

[60] Binbin Xie, Jie Xiong, Xiaojiang Chen, Eugene Chai, Liyao Li, Zhanyong Tang, and Dingyi Fang. Tagtag: material sensing with commodity rfid. In *Proceedings of the 17th Conference on Embedded Networked Sensor Systems*, SenSys '19, page 338–350, New York, NY, USA, 2019. Association for Computing Machinery.

[61] Lei Yang, Yekui Chen, Xiang-Yang Li, Chaowei Xiao, Mo Li, and Yunhao Liu. Tagoram: real-time tracking of mobile rfid tags to high precision using cots devices. In *Proceedings of the 20th Annual International Conference on Mobile Computing and Networking*, MobiCom '14, page 237–248, New York, NY, USA, 2014. Association for Computing Machinery.

[62] Zhixiong Yang, Ziyi Zhen, Hui Xu, Yajun Zhang, and Xinlong Feng. Rf-ui: Continuous user identification through gaits using rfid. *IEEE Transactions on Cognitive Communications and Networking*, 2024.

[63] Jiangjin Yin, Xin Xie, Hangyu Mao, and Song Guo. Efficient missing key tag identification in large-scale rfid systems: An iterative verification and selection method. *IEEE Transactions on Mobile Computing*, 2024.

[64] Shihao Yin and Liang Dong. Plant tattoo sensor array for leaf relative water content, surface temperature, and bioelectric potential monitoring. *Advanced Materials Technologies*, 9(12):2302073, 2024.

[65] Sangki Yun, Yi-Chao Chen, Huihuang Zheng, Lili Qiu, and Wenguang Mao. Strata: Fine-grained acoustic-based device-free tracking. In *Proceedings of the 15th annual international conference on mobile systems, applications, and services*, pages 15–28, 2017.

[66] Pengyu Zhang, Dinesh Bharadia, Kiran Joshi, and Sachin Katti. Hitchhike: Practical backscatter using commodity wifi. In *Proceedings of the 14th ACM conference on embedded network sensor systems CD-ROM*, pages 259–271, 2016.

[67] Pengyu Zhang, Colleen Josephson, Dinesh Bharadia, and Sachin Katti. Freerider: Backscatter communication using commodity radios. In *Proceedings of the 13th international conference on emerging networking experiments and technologies*, pages 389–401, 2017.

[68] Jia Zhao, Wei Gong, and Jiangchuan Liu. Microphone array backscatter: an application-driven design for lightweight spatial sound recording over the air. In *Proceedings of the 27th Annual International Conference on Mobile Computing and Networking*, MobiCom '21, page 710–722, New York, NY, USA, 2021. Association for Computing Machinery.

[69] Feng Zhou, Chunhong Chen, Dawei Jin, Chenling Huang, and Hao Min. Evaluating and optimizing power consumption of anti-collision protocols for applications in rfid systems. In *Proceedings of the 2004 International Symposium on Low Power Electronics and Design (IEEE Cat. No.04TH8758)*, pages 357–362, 2004.

A APPENDIX A: CIRCUIT DESIGN: ADAPTING TO FLEXIBLE REFERENCE FREQUENCIES

A constant current source is implemented with a PNP transistor Q_2 whose *emitter* connects to the power supply V_{sup} through a tunable resistor R_{set}, *base* connects to a stable voltage reference V_Z (e.g., a zener diode), and *collector* charges a capacitor C. The charging current is $I_{ch} = \frac{V_{sup} - V_Z - V_{BE}}{R_{set}}$, where V_{BE} denotes the *base-emitter* voltage drop of the transistor. Therefore, the charging voltage $V_c(t)$ across the capacitor C follows the linear relationship by time t:

$$V_c(t) = I_{ch} \cdot t/C = \frac{V_{sup} - V_Z - V_{BE}}{R_{set}} \cdot t/C \qquad (6)$$

It shapes a linear rise within the period of the timing reference. To ensure the same intended amplitude output voltage V_{max} is produced at any frequency, the value of R_{set} should be adjusted according to the reference frequency f_{env}. In practice, the value of R_{set} can be determined refer to Eqn. 6 as following:

$$R_{set} = \frac{V_{sup} - V_Z - V_{BE}}{f_{env} \cdot V_{max} \cdot C} \qquad (7)$$

B APPENDIX B: VCO DETAILS

Fig. 15 shows the VCO schematic. The output frequency f_{out} of the VCO varies between $488Hz$ and $1MHz$ based on V_{out}, following:

$$f_{out} = \frac{1MHz \cdot 50k}{N_{DIV} \cdot R_{VCO}} \cdot (1 + \frac{R_{VCO}}{R_{SET}} - \frac{V_{out}}{V_{SET}}) \qquad (8)$$

where N_{DIV} is a programmable divider that controls the division ratio of the output frequency and is set to 1, and V_{SET} is typically set to $1V$.

C APPENDIX C: DECODING ALGORITHMS

We list the details of the tracking frequency algorithm and the FSM decoding algorithms below:
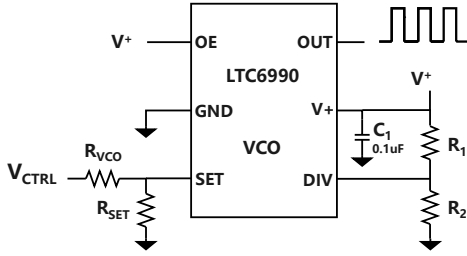
D APPENDIX D: SENSOR

Figure 15: VCO used by MmBack.

Algorithm 1: Find Decrease Points

Input: slice: Magnitude variation of f_i
Output: Decrease points

1   derivative ← ∇ slice ;
2   peaks ← find_peaks(derivative, height = threshold) ;
3   Initialize decrease_points as empty list ;
4   **foreach** peak *in* peaks **do**
5   search ← peak - 1 ;
6   **while** derivative[search] ≤ gradient_threshold **and** search > *0* **do**
7   search ← search - 1 ;
8   Append search to decrease_points ;
9   **return** decrease_points

Algorithm 2: Decode

Input : signal: collected signal, F: frequency levels, N: CZT window size, M: CZT frequency bins, C: number of sensors, start: start frequency of CZT, end: end frequency of CZT, mask: a matrix of 0 and 1 to sum up duty cycles for each sensor
Output: readings: sensor readings $R_1, \ldots, R_C$

1   steps ← len(signal) − N +1 ;
2   spectrograms ← [ ] ;
3   **for** i ← 0 *to* steps *do* **do**
4   spec ← CZT(signal[$i : i + N$], M, start, end) ;
5   Append spec to spectrograms ;
6   periods ← Algorithm1(spectrograms[F_0]) ;
7   durations ← [ ] ;
8   **for** i ← 0 *to* len(periods) - 1 **do**
9   slice ← spectrograms[periods[i]:periods[$i + 1$]] ;
10   transitions ← Algorithm1(slice[F]) ;
11   **for** j ← 0 *to* C **do**
12   selected_frequency ← argmax(slice[F_j]) ;
13   Append transitions[selected_frequency] to durations ;
14   **return** durations × mask;

Table 3: Sensor Specifications

Sensor	Part Number	Manufacturer
Water Level	4965	Adafruit Industries LLC [2]
Soil Moisture	SEN0114	DFRobot [13]
Temperature	-	Arduino [5]
Light	-	Arduino [5]
Microphone	-	Arduino [5]
PPG	SEN0203	DFRobot [14]
ECG	SEN0213	DFRobot [15]
ABP	MPS20N0040D-S	Reland Sun [34]
RESP	SFM3020	Sensirion AG [45]